QUARTERLY REPORT

(Data Item A002)

mccrone associates, inc.

850 PASQUINELLI DRIVE • WESTMONT, ILLINOIS 60559 • 312-887-7100

ARPA Order Number:

Contract Number: F08650-94-C-0034

Effective Date of Contract: 28 February 1994

Reporting Period: 1 Sep thru 30 Nov 94

Principal Investigator: Stephen B. Rice, PhD
708-887-7100

QUARTERLY REPORT

(Data Item A002)

Date: 19 December 1994

MA Number: 22319

Copy 4 of 10

Sponsored By:

Advanced Research Projects Agency

ARPA Order No.

Monitored by_____

Agent_____

under Contract F08650-94-C-0034

mcrone associates, inc.
850 PASQUINELLI DRIVE • WESTMONT, ILLINOIS 60559

ANALYTICAL ELECTRON MICROSCOPY OF NANOMETER-SIZED PARTICLES

Quarterly Report No. 3

for the period 1 September 94 thru 30 November 94

F08650-94-C-0034

AFTAC Project Authorization T/3420

(CDRL Data Item A002)

I. INTRODUCTION

During the past quarter, despite lengthy downtime for the JEOL 4000FX, two aspects of our research plan were initiated: microdiffraction and the the effects of prolonged beam exposure on the EELS signature of U oxides. While obtaining microdiffraction patterns, it was recognized that high resolution electron microscope images can be obtained on thin sections produced by ultramicrotomy.

II. TECHNICAL PROGRESS

A. Task 3.2.1-1 Evaluation of Brightfield/Darkfield Imaging

Efforts under this task will be initiated during the Fourth Quarter.

B. Task 3.3.1 Actinide Analyses Using Diffraction Techniques

One of the aims of this research is to study whether microdiffraction (μD) techniques can routinely identify nanometer-sized particles. In the September '94 Quarterly report, we discussed some of the factors influencing the diffraction characteristics of uranium oxides when they occur in polycrystalline forms. Crystallographic details such as atom positions, disorder, nonstoichiometry, and chemical bonding are characteristics that determine the information available for 'fingerprinting.' Microdiffraction studies on thin-sections and fine particles may help us understand these patterns. Figure 1 is a μD pattern from a 50Å crystallite of U_3O_8. It is oriented down the [100] axis, and the convergence of the beam is set so the disks nearly touch. Despite being formed by a ~50Å diameter beam, this is not entirely from one crystal, as extra disks are visible. Figure 2 is a high resolution image of U_3O_8 showing typical crystallites in an aggregate, and from one of which the pattern in Fig. 1 was taken. The average size is about 30-50Å, and the lattice fringes are clearly visible.

Figure 3 shows a UO_2 aggregate consisting of fewer, but much larger crystallites. The prevalent set of lattice fringes that run NW-SE across the particle indicate that the aggregate is dominated by one crystallite.

Figure 4 shows a small thin edge of another crystallite. Accurate information from microdiffraction patterns demands that the section be only one crystallite thick (e.g. for UO_2 about 250Å and for U_3O_8 about 50Å). In this case the region is actually thinner than the average section thickness.

These results suggest that HREM is an additional route to characterizing thin sections. For example, the variation of lattice fringes from one grain to another in a suitably thin region could be rapidly assessed. This will provide a kind of map of crystallinity, which, for many specimens, will show crystalline versus non-crystalline portions. In this part of the study we are using only relatively pure reference materials. The real utility will be tested when the specimens are more complicated mixtures or poorly characterized oxides.

C. Task 3.3.2 Component Analysis of Large Particles Using Micro-diffraction

Efforts under this task will be initiated during the Fourth Quarter.

D. Task 3.4.1 EELS Near-Edge Structure Analysis of Actinides

A study was made of EELS spectra for two TiO_2 polymorphs, rutile and anatase mineral specimens. Having the same composition, and in particular identical oxidation state, but contrasting crystal structures, they give a comparison for how important crystal structure might be in controlling EELS near edge structure. In principle, the two phases may be distinguishable, provided the resolution is good enough. The energy resolution for the 4000FX with the Gatan PEELS spectrometer is about 1-1.5 eV. Apparently this is not sufficient because in our example they are essentially the same. Figure 5 shows the Ti $L_{2,3}$ edge region for both polymorphs. One conclusion drawn from the similarity is the effects of bond type, strength, and angle: although these cannot be ruled out, they may be less important in the near edge structure than is oxidation state.

In the Sept '94 Quarterly report, we discussed an EELS peak at 16 eV, and whether it represents a surface plasmon, a thickness effect, or the consequence of sample exposure to the electron beam. One test of variation across a thin-section was made for areas a-f of the region of U_3O_8 (C-533) shown in Figure 6. The darker areas are dark for one of two reasons, either thickness differences due to overlap or diffraction contrast. EELS low loss results for spectra d, e, and f are compared. Spectrum e is from a curled region, and therefore twice as thick as the others. Spectra from areas d and f are very similar, but e has a broader low loss intensity distribution. The main difference is the intensity of the 35 eV feature in this region, which includes the plasmon. The 35 eV feature is different than the 16 eV feature, and probably relates directly to plural scattering as a result of greater thickness.

Table 1 gives measurements of single-thickness for typical regions of slices analyzed by EELS. Two values of t/Λ (from the zero loss peak to plasmon intensity ratio) were obtained sequentially for each region analyzed. The difference between them can be as great as $\pm 15\%$. The thickness value reported is for the average of the two EELS measurements. The low loss region was also studied in more detail in terms of prolonged beam exposure (See 3.4.2 below).

Table 1. Comparison of thickness estimates from EELS data for UO_2 (C-531) and U_3O_8 (C-533). [Two spectra, each about 10 readouts of 1 sec integration time, were recorded in sequence. Microscope operating conditions: 350 kV, 0.5 eV/channel, 2 mm aperture, image mode.]

Analysis #	Sample	t/Λ	thickness t, nm
1	UO_2 (C-531)	0.985, 0.964	38
2	UO_2	0.940, 1.083	39
3	UO_2	0.879, 0.888	34
4	UO_2	0.856, 0.848	33
5	UO_2	0.861, 0.883	34
6	U_3O_8 (C-533)	0.801, 0.753	30
7	U_3O_8	0.796, 0.781	31
8	U_3O_8	0.745, 0.723	29
9	U_3O_8	0.587, 0.655	24
10	U_3O_8	1.035, 1.104	42

E. Task 3.4.2 Effects of Prolonged Beam Exposure

Slices of both UO_2 and U_3O_8 were analyzed at constant beam conditions for different durations. The conditions used were an accelerating voltage of 350 kV, current density of about 12 pA/cm^3, and 0.5 sec integrations

taken at the intervals indicated on the plots. Lesser or greater current density is the most crucial parameter because it determines the effective dose impinging on the specimen. From observation of selected area electron diffraction patterns, it was noted in these experiments that the crystallinity of the specimens remained intact during the entire period of beam exposure. In later experiments we will vary the dose so crystallinity is lost during the early and late stages of the experiment. If the oxide were to become non-crystalline, this should cause a measurable change in the EELS spectrum, and dose variation provides another way of controlling the parameters in the specimen as well as in the microscope.

Because the low loss region is of most interest for fingerprinting the oxidation state, this energy range was investigated first. Figures 7 and 8 show two results for UO_2 and one for U_3O_8, respectively. In several experiments of prolonged exposure, the main effect was the growth of the 16 eV feature. Under the conditions used for these experiments, measurable intensity appears in the spectrum after several minutes of exposure, and a pronounced feature is visible. The time interval during which the 16 eV feature becomes comparable in intensity to the main plasmon peak is about 100 minutes in Figure 7a, whereas in 7b this happens after only 20 minutes. Note that the two areas had very similar zero-time spectra. Because the regions were analyzed with a ~100 nm spot, several grains were included. Smaller spot sizes could be used. The question of orientation dependence of an EELS spectrum will be tested by collecting spectra from individual crystallites whose orientation is determined from microdiffraction.

The 16 eV peak appears to be related to intrinsic characteristics of the less oxidized phases, as well as a response to changes in valence introduced by the electron beam during analysis.

F. Task 3.5.1 Investigation of EELS Mapping

Due to delays caused by instabilities in the high voltage on the 4000FX instrument, no progress was made in this area of research. Efforts under this task will be initiated during the Fourth Quarter.

III. PROBLEMS ENCOUNTERED

The JEOL 4000FX AEM, the primary instrument for EELS studies under this contract, continued to experience high voltage instability, especially at accelerating voltages above 300 kV. This required maintenance during much of the Third Quarter. A new gun assembly was installed toward the end of this quarter, and troubleshooting to find the source of the instability continues. Installation of the new gun has not entirely solved the problem.

IV. TRAVEL

No travel was done during the Third Quarter.

V. CONTRACT PERFORMANCE STATUS

The Gatan DigiScan (hardware and software) for acquiring STEM images was installed, and is now fully operational.

Due to the downtime experienced this quarter, we are behind in the hourly effort and billing expected for this time in the contract schedule.

FIGURE CAPTIONS

1. Microdiffraction pattern obtained from 50 Å crystallite of U_3O_8 (C-533), [100] projection.

2. High resolution TEM brightfield image of a microtome preparation of U_3O_8 (C-533).

3. High resolution TEM brightfield image of a microtome preparation of UO_2 (C-531).

4. High resolution TEM brightfield image of a microtome preparation of UO_2 (C-531).

5. Comparison of EELS Ti $L_{2,3}$ edge spectra for anatase and rutile.

6. Comparison of EELS spectra obtained from areas d, e, and f of U_3O_8 (C-533) slice in the image inset.

7. Sequential EELS spectra for two regions of a microtomed preparation of UO_2 (C-531), showing the development of a pronounced peak on the low energy side of the plasmon peak, at about 16 eV. Numbers on spectra refer to minutes of exposure.

8. Sequential EELS spectra for one region in a microtome preparation of U_3O_8 (C-533), also showing the development of a peak at 16 eV. Numbers on spectra refer to minutes of exposure.

Figure 1

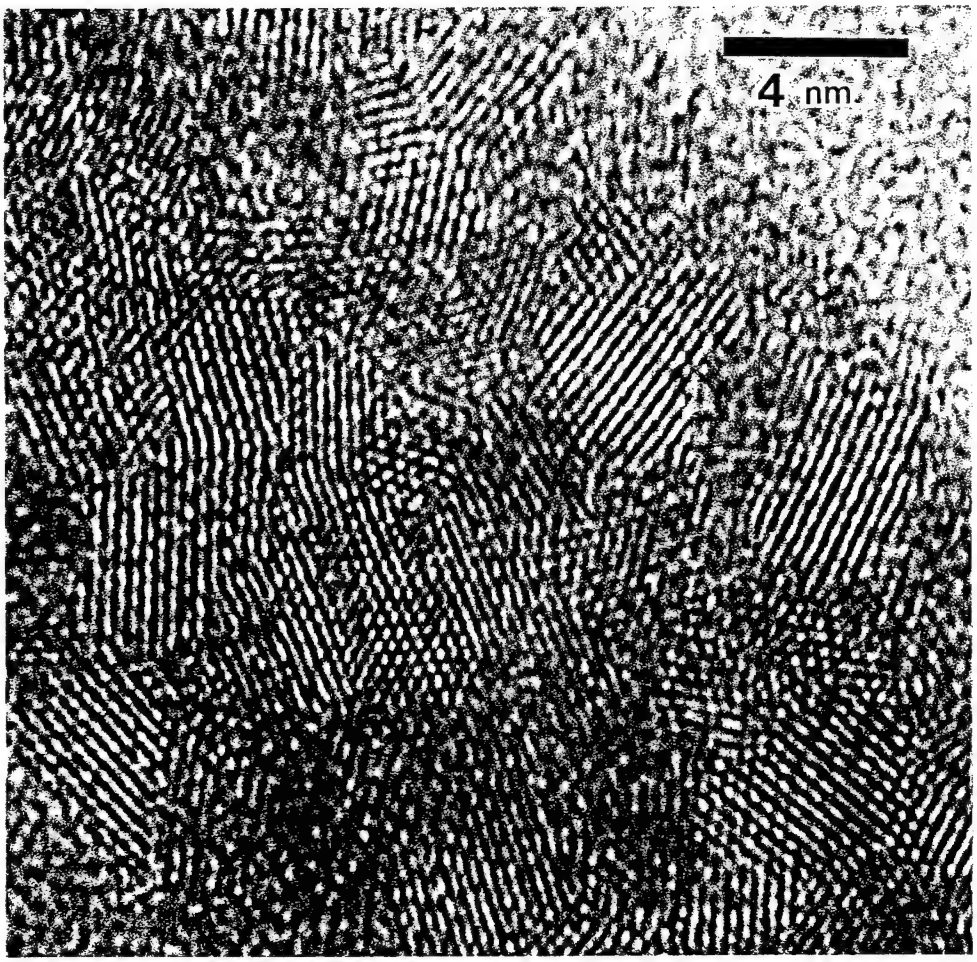

Figure 2

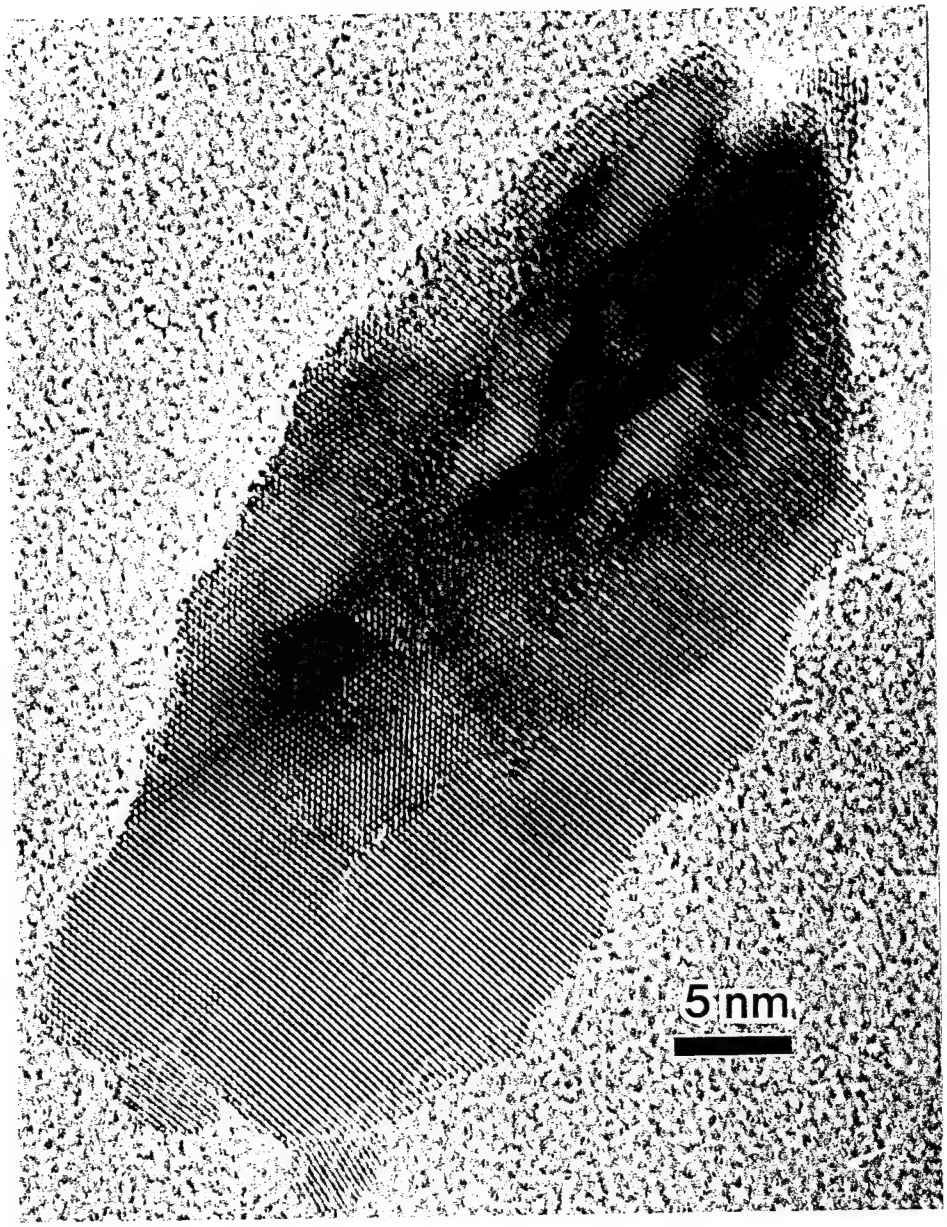

Figure 3

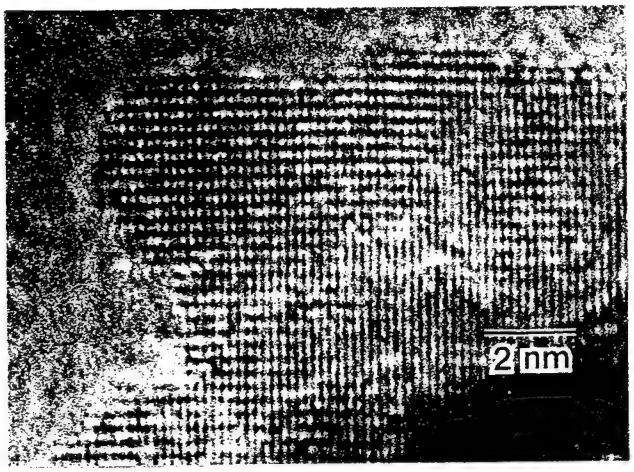

Figure 4

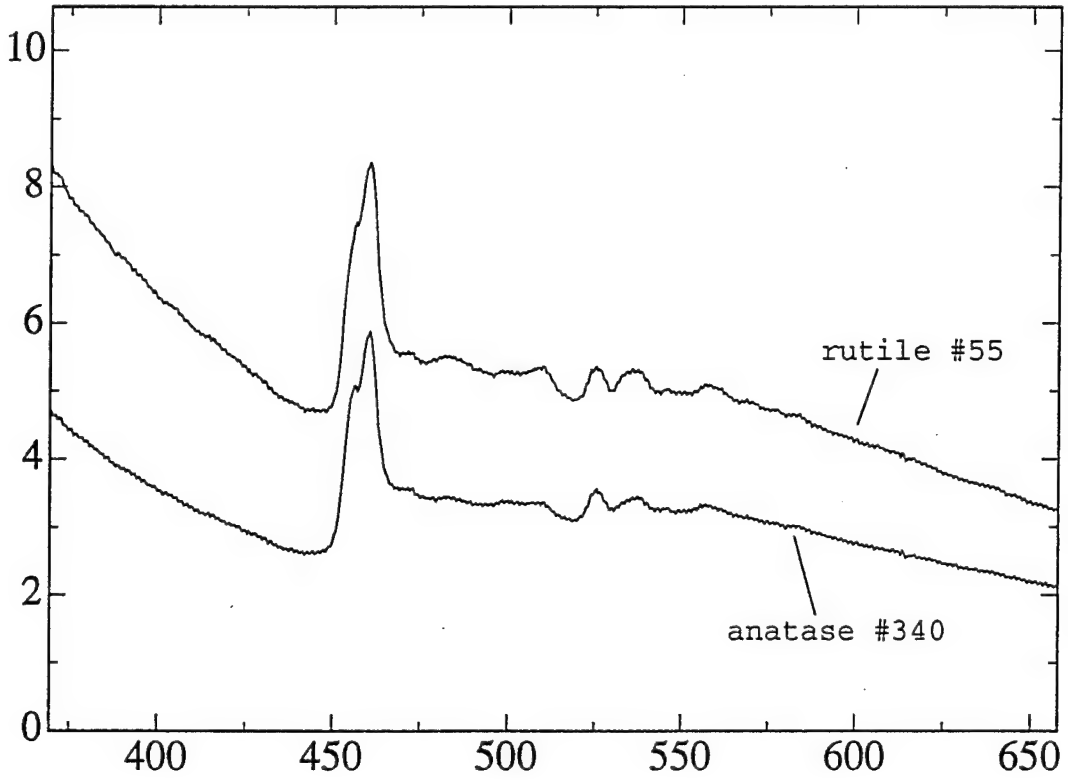

Figure 5

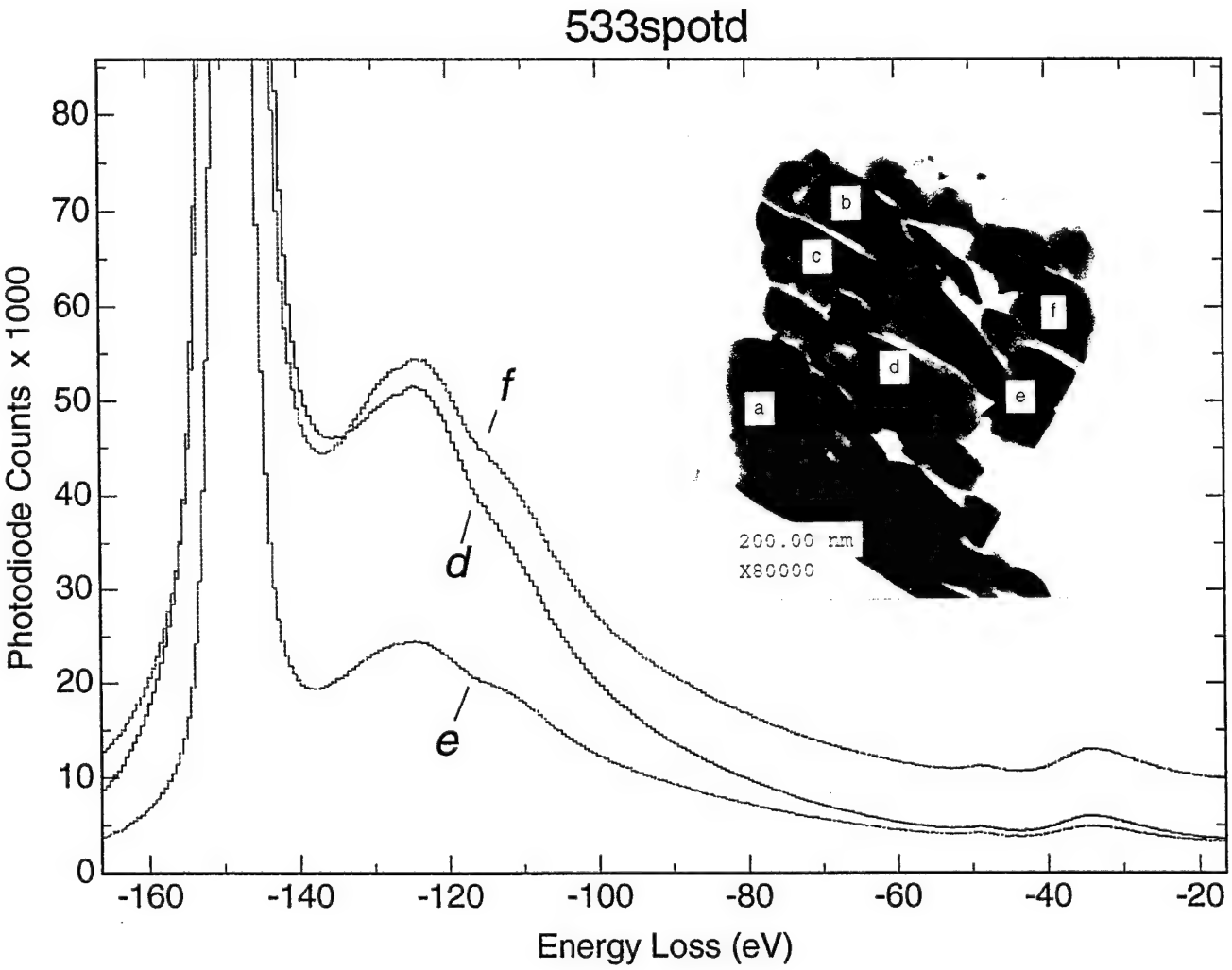
533spotd
Photodiode Counts x 1000
80
70
60
50
40
30
20
10
0
-160
-140
-120
-100
-80
-60
-40
-20
Energy Loss (eV)
f
d
e
a
b
c
d
e
f
200.00 nm
X80000

Figure 6

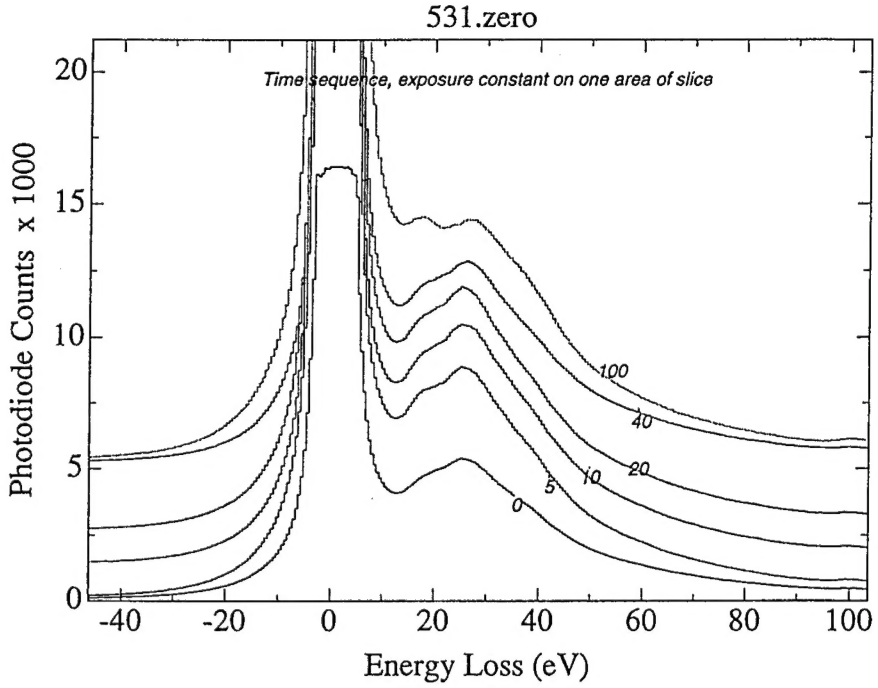

Figure 7a

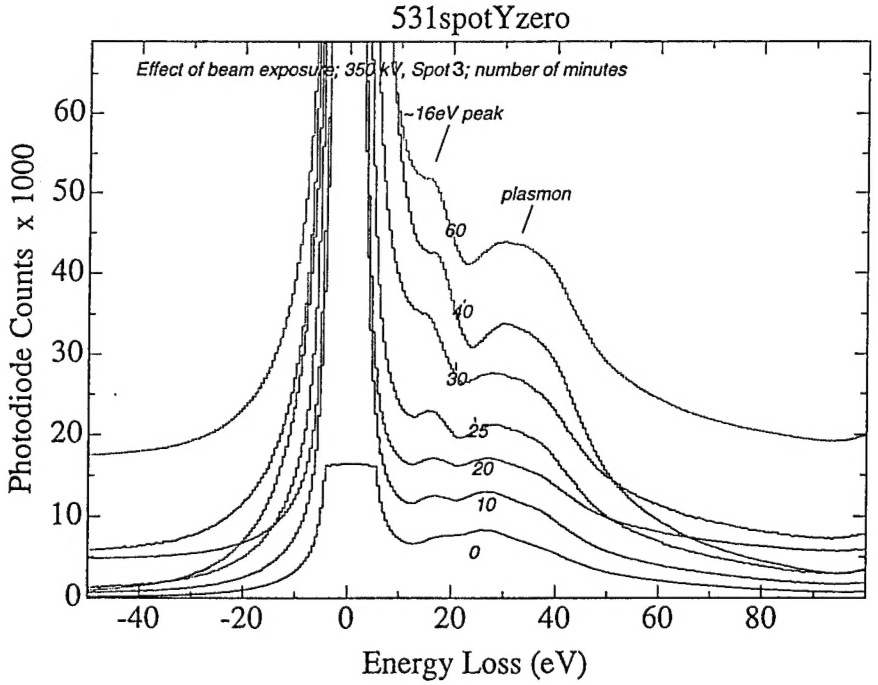

Figure 7b

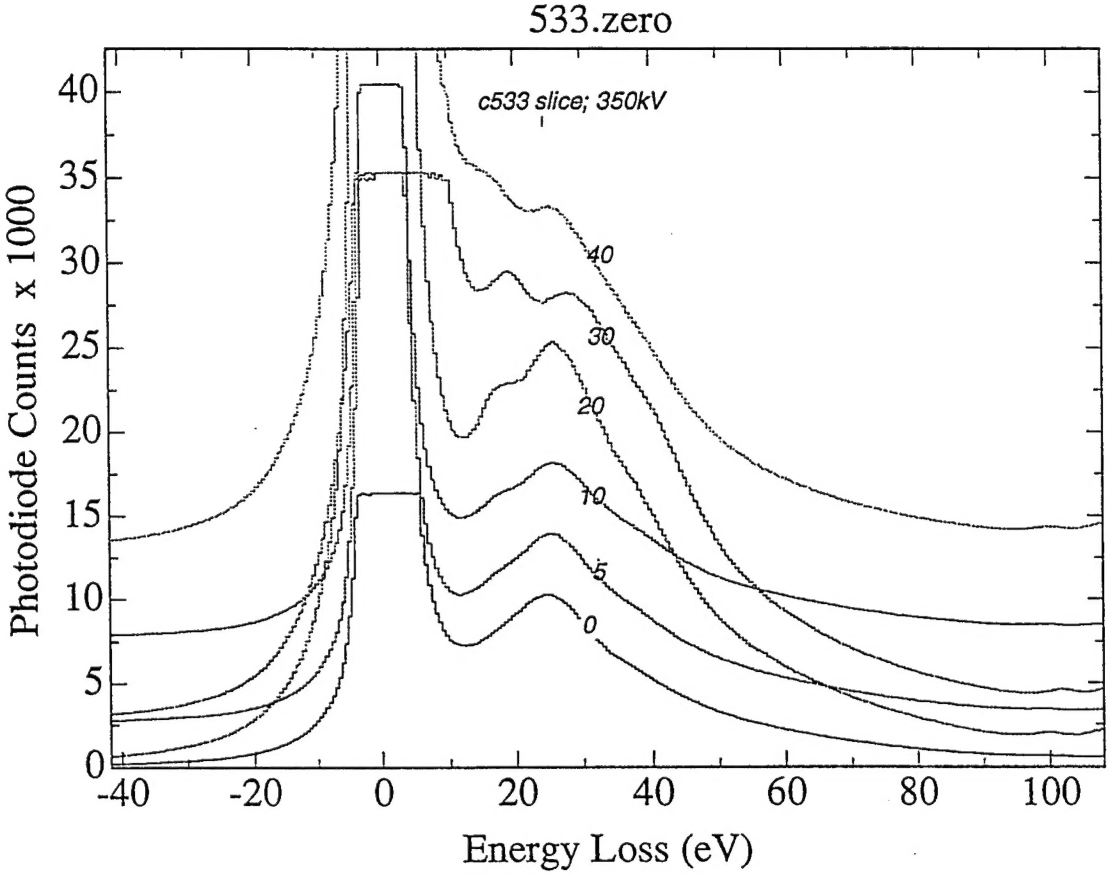
533.zero
c533 slice; 350kV
40
30
20
10
5
0
Photodiode Counts x 1000
0
5
10
15
20
25
30
35
40
-40
-20
0
20
40
60
80
100
Energy Loss (eV)

Figure 8

APPENDIX A

CONTRACT PERFORMANCE STATUS

ANALYTICAL ELECTRON MICROSCOPY OF NANOMETER-SIZED PARTICLES: CONTRACT F08650-94-C-0034
CONTRACT PERFORMANCE STATUS (ESTIMATED)
CUMULATIVE AS OF 30 NOVEMBER 1994

CONTRACT PERIOD OF PERFORMANCE 28 FEB 1994 thru 28 FEB 1996

		TASK BREAKDOWN BY HRS	BUDGETED HOURS	EXPENDED HOURS	% HOURS EXPENDED	BUDGETED FUNDS *	EXPENDED FUNDS	% FUNDS EXPENDED	WEIGHTED VALUE	% WORK COMPLETED (HOURS)	% TOTAL COMPLETED (HOURS)
TASK 3.2.1-1 (CLIN 0001AA)	Evaluation of BRIGHTFIELD/ DARKFIELD imaging	11.9%	398	20.5	5.2%	43,133	1,935	4.5%	0.119	1%	0.1%
TASK 3.3.1 (CLIN 0001AB)	Actinide analyses using different diffraction techniques	13.8%	463	70	15.1%	50,208	6,936	13.8%	0.138	15%	2.1%
TASK 3.3.2 (CLIN 0001AB)	Component analysis of large particles using micro-diffraction	9.3%	313	4	1.3%	33,949	393	1.2%	0.093	2%	0.2%
TASK 3.4.1 (CLIN 0001AC)	Near edge structure analysis of actinides	22.0%	738	267	36.2%	70,353	28,091	39.9%	0.220	35%	7.7%
TASK 3.4.2 (CLIN 0001AC)	Effects of prolonged beam exposures	11.3%	378	11	2.9%	36,033	1,104	3.1%	0.113	5%	0.6%
TASK 3.5.1 (CLIN 0001AD)	Investigation of EELS mapping	18.7%	628	10	1.6%	67,530	1,257	1.9%	0.187	0%	0.0%
OTHER DIRECT COSTS (CLIN 0001AE)						66,118	38,797				
CDRL's (CLIN 0002)		13.0%	436	91.75	21.0%	61,442	15,602	25.4%	0.130	6%	0.8%
TOTALS		100.0%	3,354	474	14.1%	428,766	94,114	22.0%	1.000		11.4%

*NOTE: The contract combines Tasks 3.3.1 and 3.3.2 under CLIN 0001AB and Tasks 3.4.1 and 3.4.2 under CLIN 0001AC. Therefore the Budgeted and Expended are estimated based upon a proration of Budgeted Hours.